JOURNAL OF CATALYSIS **174,** 142–152 (1998)
ARTICLE NO. CA981957

Identification of the Active Sites in the Selective Hydrogenation of Acetic Acid to Acetaldehyde on Iron Oxide Catalysts

R. Pestman,* R. M. Koster,* E. Boellaard,† A. M. van der Kraan,† and V. Ponec*,[1]

**Leiden Institute of Chemistry, Leiden University, Gorlaeus Laboratories, P.O. Box 9502, 2300 RA Leiden, The Netherlands; and †Interfacultair Reactor Instituut, Delft University of Technology, Mekelweg 15, 2629 JB Delft, The Netherlands*

Received June 23, 1997; revised October 22, 1997; accepted October 22, 1997

Iron-based catalysts appeared to be very active and selective in the hydrogenation of acetic acid to acetaldehyde. The active and selective catalyst consists of a metallic and an oxidic phase. Probably, the metal is needed to activate hydrogen, and the oxide is needed to provide the reaction site for the selective hydrogenation. Catalyst pretreatment and reaction conditions must be carefully controlled: the catalyst must be prereduced and the hydrogen/acid ratio must be higher than four. Only then are both iron-containing phases formed and kept stable during the reaction. The function of hydrogen is twofold: it must keep the catalyst in its active, partly reduced, form and it acts as reactant in the hydrogenation of acetic acid. © 1998 Academic Press

INTRODUCTION

Aldehydes are frequently used, as either intermediates in various syntheses or directly as flavors and fragrances. As carboxylic acids are easy to synthesize or readily available, it is attractive to develop a clean and cheap way to produce aldehydes from carboxylic acids. Until recently, this only succeeded for the production of aromatic aldehydes (1–7), and not for aliphatic acids. However, previous research at the Leiden University, using small aliphatic acids as model compounds, showed that it is possible to hydrogenate directly in a catalytic way aliphatic acids to their corresponding aldehydes (8–13).

The results obtained during the study of the hydrogenation of acetic acid to acetaldehyde with different oxidic catalysts show a clear dependence of the selectivity to acetaldehyde on the metal–oxygen bond strength of the catalysts (8, 10). Oxides with a low metal–oxygen bond strength have a low selectivity for the reaction of acetic acid to acetaldehyde. The same is true for oxides with a high bond strength. Intermediate cases, such as the oxides of tin and iron and to a lesser extent the oxides of vanadium and germanium, have a high aldehyde selectivity. Hence, a plot of selectivity versus metal–oxygen bond strength results in a volcano-shaped curve. This dependence can be explained by assuming that the selective hydrogenation to aldehyde takes place via a Mars and Van Krevelen type of mechanism, where lattice oxygens, and thus also oxygen vacancies, participate in the reaction.

When platinum is added to the oxidic catalysts, the above described picture changes with respect to certain points (10). The volcano-shaped plot of the selectivity versus the metal–oxygen bond strength remains unaltered, but the overall selectivity for acetaldehyde is higher. A higher yield is seen for all hydrogenation and hydrogenolysis reaction products—thus not only for acetaldehyde, but also for ethane, methane, and water. All these hydrogen-consuming reactions run at lower temperatures than the reactions occurring on pure oxides. Since the volcano-shaped correlation persists after addition of platinum to the catalysts, the reacion probably still proceeds via the same mechanism. In addition to that, the activity of the Pt/titania catalyst appeared to be dependent on the amount of oxide used and not on the amount of platinum (10). Thus, the reaction likely takes place on the oxide and not on the metal. The main role of platinum is presumably to activate molecular hydrogen, which can migrate via spillover to the oxide. This explains why both the selectivity increases and the reaction temperature decreases when platinum is added.

It is noteworthy that acetone formation, which is the most important side reaction on pure oxides, is suppressed completely by the addition of platinum. The production of acetone needs no hydrogen and, therefore, occurs readily on pure oxides. The presence of platinum-activated hydrogen probably favors hydrogenation reactions at the cost of the ketonization reaction, which is initiated by a *de*hydrogenation step (11).

Iron oxide proved to have the highest selectivity of all pure oxides (10) provided that a certain way of preparation was followed. Therefore, it is interesting to investigate the iron oxide catalyst more closely. Morever, several unanswered questions arise when analyzing the catalytic behavior of this oxide. For instance, the exact composition

---

[1] To whom correspondence should be addressed. Fax: ++31 71 5274451.

0021-9517/98 $25.00

of the catalyst under reaction conditions is not clear, addition of platinum does not influence selectivity much (10), and the selectivity is strongly dependent on pretreatment conditions.

A closer inspection of the literature also suggests that there is, indeed, a pronounced dependence of the selectivity on the pretreatment, reaction conditions, and the acid used. Two patents claim that the selective hydrogenation to aldehydes over iron oxide is only possible when the carboxylic acid contains at most one α-hydrogen atom (14, 15). Indeed, it has been reported that acetic acid, which has three α-hydrogen atoms, undergoes ketonization—instead of hydrogenation—on iron oxide, even in the presence of hydrogen (16, 17). However, all the above-mentioned sources of information—patents and open literature—mention the use of a hydrogen/acid ratio of not more than 4 and do not mention any influence of prereduction. In this case, the most abundant phase of the catalyst during the reaction is presumably Fe_3O_4. Hindermann *et al.* reported that, when a hydrogen/acid ratio of 10,000 was used and the catalyst was prereduced, an iron catalyst yielded 28% acetaldehyde. The selectivity could be increased further by the addition of a potassium compound as a promoter to the catalyst. After reaction the pure iron catalyst contained 94.6% metallic iron and the promoted (improved) catalyst only 85.4% (18, 19).

In a preliminary report presented earlier (13), a speculative explanation is given describing the behavior of iron oxide as a catalyst for the selective hydrogenation of acetic acid to acetaldehyde. In this paper a closer look is taken at the behavior of iron oxide and at the influence of pretreatment and reaction conditions. Additionally, *in situ* Mössbauer spectrometry measurements have been performed to characterize the catalysts.

METHODS

The catalytic experiments with acetic acid were performed in a flow system at slightly elevated pressure (total pressure: 1.2 bar). A hydrogen (90 ml/min) or helium (118 ml/min) flow was saturated with acetic acid at room temperature (saturation pressure of about 25 mbar). Any prereduction of catalysts was done *in situ* for 4 h directly before the actual experiment. During the reaction, the temperature was raised from room temparature to 450°C at a rate of 7°C/min. Details of the set-up, measurement procedures, and analysis methods have been described earlier (10).

The iron oxide used was untreated α-Fe_2O_3 obtained from Fluka (Switzerland). For comparison, a homemade α-Fe_2O_3 was prepared by dissolving $Fe(NO_3)_3$ in water and subsequent precipitation with NH_4OH. The precipitated $Fe(OH)_3$ was washed with water, ethanol, and ether and subsequently calcined at 625°C for 24 h. The parameter selectivity (S) for product i is defined as

$$S_i\ (\%) = \frac{p_i c_i}{\sum_{\text{products}} p_i c_i} \cdot 100\%,$$

where p_i is the partial pressure and c_i is the number of carbon atoms of product i.

In this paper, the oxidation state of the iron catalysts during the prereduction and the reaction was determined by Mössbauer spectroscopy using an *in situ* Mössbauer reactor (20). The prereduction of the catalysts was performed in a 10% H_2 in Ar flow. For the hydrogenation of acetic acid the gas stream (20 ml/min) was saturated with acetic acid (25 mbar) and subsequently led over the catalysts at constant temperature. Mössbauer spectra were recorded using a ^{57}Co in Rh source. The spectrometer was operated in the constant acceleration mode with a symmetric, triangular velocity wave form. The obtained set of mirrored spectra was matched in order to eliminate the curved background due to the varying distance between source and detector. The Mössbauer parameters isomer shift (IS), quadrupole splitting (QS), effective hyperfine field (H_{eff}), line width (Γ), and the spectral contribution (SC) were determined by fitting the spectra with subspectra consisting of Lorentzian-shaped lines using a nonlinear iterative minimization routine. In case of quadrupole doublets, the line widths as well as the absorption areas were constrained to be equal for both lines. Isomer shifts are reported with respect to the NBS standard sodium nitroprusside. The hyperfine field was calibrated with the 515 kOe field of α-Fe_2O_3.

RESULTS

The Influence of Pretreatment

Pure α-Fe_2O_3 was used as a catalyst in the temperature-programmed reaction of acetic acid with hydrogen (Fig. 1). The reaction started at about 340°C and acetone, acetaldehyde, water, CO_2, and CO were the main products. When the same catalyst was used again in a similar temperature-programmed reaction, the reaction started at lower temperatures and more acetaldehyde was formed.

The following tests were performed to examine what caused the difference in catalytic behavior between a fresh and a used catalyst. First, the influence of carbon deposition was tested. Deposition of carbon from acetylene or ethylene did, however, not increase the selectivity. Addition of carbonates to the surface showed the same lack of positive influence. However, a rather severe prereduction of the iron oxide was beneficial for the steady-state selectivity of the catalyst (Fig. 2).

In Fig. 3 the maximum obtainable selectivity to acetaldehyde is plotted as a function of the prereduction temperature. All these selectivities were obtained at yields higher than 80%. The highly selective catalysts—prereduced at

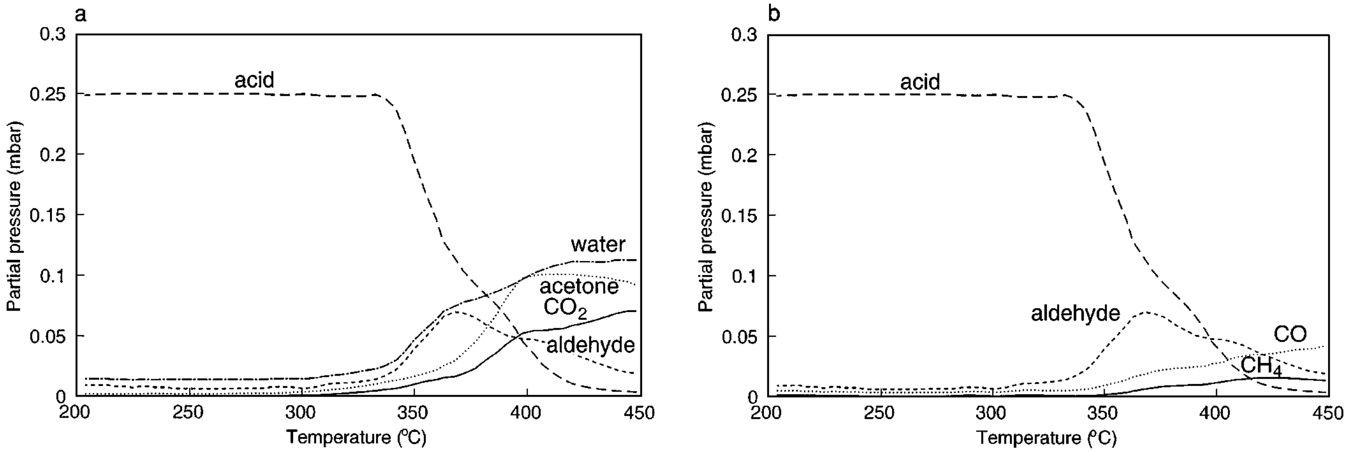

FIG. 1. Acetic acid and its reaction products over an α-Fe_2O_3 catalyst. (N.B., for the sake of clarity, the various products are shown in two figures and compared to the same standards—acetaldehyde and acetic acid).

450, 500, and 600°C—produce only aldehyde and alcohol (together they account for almost 100% of all products). The catalyst reduced at 700°C produces also a lot of methane. X-ray diffraction patterns showed that below 400°C only oxidic forms of iron were visible by this technique (Fe_2O_3 and Fe_3O_4). The catalysts reduced at 450 and 500°C consisted of both α-Fe (bcc) and Fe_3O_4; above these prereduction temperatures only α-Fe was detected by XRD.

Oxidation State during the Reaction

As shown in Fig. 3, prereduction of the iron oxide catalyst increased the selectivity to acetaldehyde. However, the reactants are able both to reduce (H_2) as well as to oxidise (acetic acid) the catalyst. The exact oxidation state of the iron during the reaction was thus unknown and had to be determined. A completely reduced iron catalyst (reduced in an H_2 flow at 700°C for 18 h) was used in a reaction of acetic acid at 350°C for 5 h. This catalyst was then subjected to a thermal-programmed desorption (TPD) in He to remove adsorbed species from the surface (Fig. 4a) and subsequently subjected to a thermal-programmed reduction (TPR) with H_2 (Fig. 4b). The results are compared with a similarly prereduced catalyst, which was not used in a reaction but to which 2 ml of oxygen was admitted at 200°C before the TPR experiment was performed. Water evolution occurred at very similar temperatures in both cases.

Mössbauer Spectroscopy

In order to get more detailed information on the composition, i.e., oxidation state, of the iron catalysts during the reaction, Mössbauer spectroscopy was used for quasi *in situ* characterization. Experiments in two flow systems were compared. One system had a mass spectrometer to

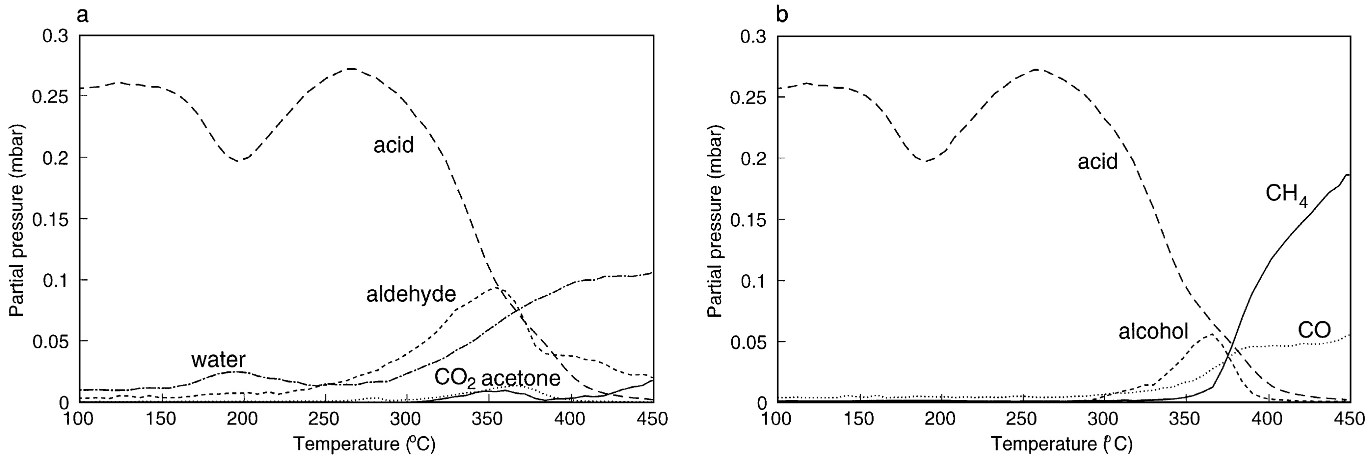

FIG. 2. Acetic acid and its reaction products over an α-Fe_2O_3 catalyst prereduced at 450°C (see N.B. at Fig. 1).

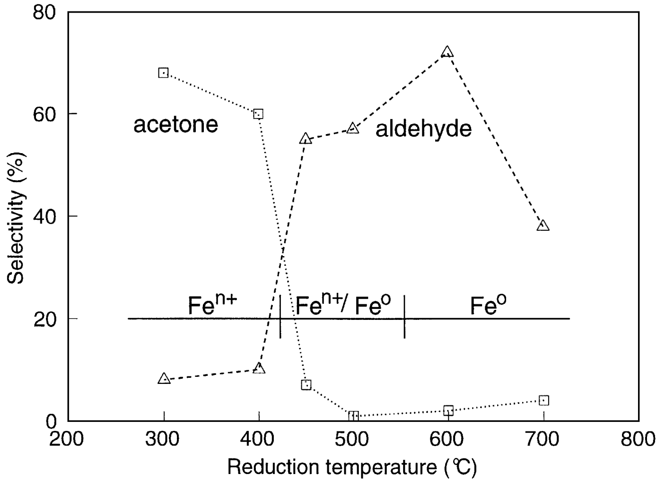

FIG. 3. Selectivity of iron catalysts plotted as a function of prereduction temperature, presented together with an indication of the phase composition as determined by XRD.

analyze the gas phase. The other system was equipped with a Mössbauer spectrometer.

First, the following experiment was performed: the catalyst was prereduced in a gas flow of 10% H_2 in He for 4 h at 450°C. After cooling down to room temperature, this flow was saturated with acetic acid and the reactor was heated to 350°C at a rate of 10°C/min. In Fig. 5, the gas-phase analysis is given from the moment the heating started. At the start, a sharp peak in the acetone production was seen, which most likely originated from acetate–salt decomposition (11). When the temperature of 350°C was reached, the catalyst produced mainly acetone. Gradual deactivation occurred, and within 10 h all the activity was lost.

Second, a series of (quasi) *in situ* Mössbauer experiments has been performed in order to determine the type of iron compounds formed during the catalytic hydrogenation process. These experiments were done with differently pretreated catalysts, i.e., an unreduced, a partly reduced (comparable with the one described above), and a completely reduced α-Fe_2O_3 catalyst. For the hydrogenation reaction a 10% H_2 in Ar flow was used, which was saturated with acetic acid at room temperature.

In Fig. 6, the Mössbauer spectra of the untreated and the partially reduced catalysts are shown, while the analysis data are presented in Table 1. After the standard reduction pre-treatment, the initially present α-Fe_2O_3 had been completely converted into a mixture of Fe_3O_4 and α-Fe (spectrum B). Besides the well-developed sexuplets of these phases, an unresolved strong background signal was recorded indicating the presence of a poorly structured magnetic phase. Exposure of this catalyst to the reaction mixture at 350°C results in a gradual conversion of the catalyst into Fe_3O_4 (spectra C and D). The *in situ* (at 350°C) recorded Mössbauer spectra exhibit again an unresolved strong resonant absorption background. After 29 h of reaction, the bulk of the catalyst had reacted to Fe_3O_4 as evidenced by the well-resolved characteristic set of sextuplets at 25°C (spectrum E). A small fraction of the catalyst

TABLE 1

Mössbauer Spectra Parameters, Reaction of Acetic Acid in 10% H_2 in He over α-Fe_2O_3

		T_m (°C)	IS (mm/s)	QS (mm/s)	H_{eff} (kOe)	Γ (mm/s)	SC (%)	Phase
A	α-Fe_2O_3	25	0.64	0.11	517	0.30	100	α-Fe_2O_3
B	After prereduction (4 h, 450°C)	25	0.54	0.01	490	0.30	15	Fe_3O_4
			0.92	−0.02	459	0.47	35	Fe_3O_4
			0.27	0.00	331	0.42	50	α-Fe
C	Between 2.3 and 6.1 h reaction at 350°C	350	0.33	−0.02	408	0.40	16	Fe_3O_4
			0.70	0.00	365	0.40	27	Fe_3O_4
			0.05	0.01	302	0.32	17	α-Fe
D	Between 22 and 29 h reaction at 350°C	350	0.35	0.00	411	0.33	21	Fe_3O_4
			0.70	−0.01	366	0.37	41	Fe_3O_4
E	After 29 h reaction at 350°C	25	0.55	0.00	491	0.28	32	Fe_3O_4
			0.93	0.00	460	0.36	64	Fe_3O_4
			0.79	0.62	—	0.30	2	Fe^{3+} (?)
			0.83	0.28	—	0.30	2	Fe^{3+} (?)
F	After oxidation by air at 25°C	25	0.54	0.00	491	0.28	32	Fe_3O_4
			0.93	0.00	460	0.36	59	Fe_3O_4
			0.80	0.59	—	0.30	5	Fe^{3+} (?)
			0.85	0.22	—	0.30	4	Fe^{3+} (?)

Note. Temperature at which the spectrum is recorded (T_m), isomer shift (IS), quadrupole splitting (QS), effective hyperfine field (H_{eff}), line width (Γ), and spectral contribution (SC).

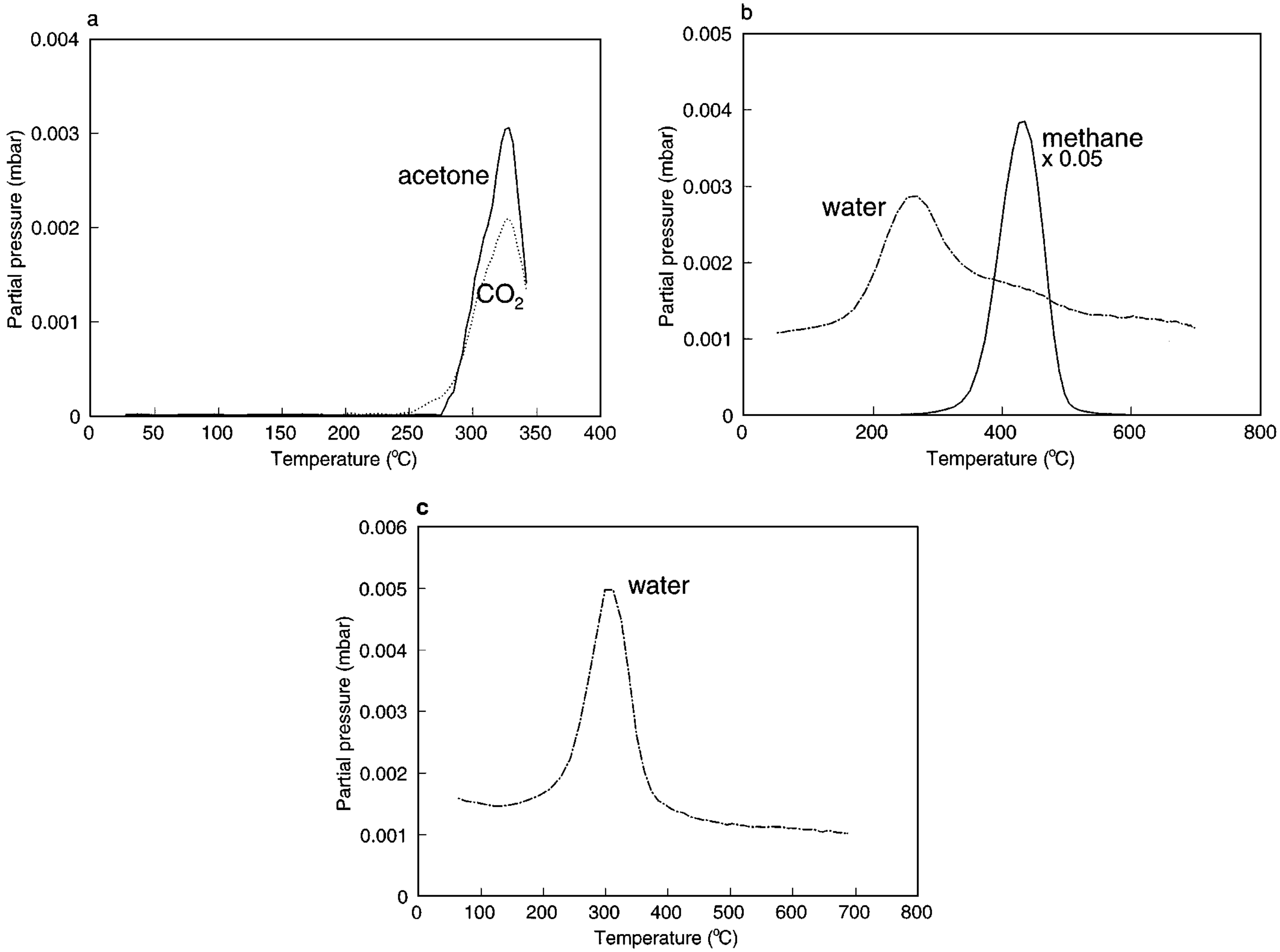

FIG. 4. (a) TPD (25–350°C) of a completely reduced iron catalyst after reaction. (b) TPR (25–700°C) of a completely reduced iron catalyst after reaction and after TPD. (c) TPR (25–700°C) of a clean iron–metal catalyst after reaction with 2 ml of oxygen.

was characterized by a poorly resolved doublet, most likely due to a Fe(III)–oxide compound. The background signal had almost completely vanished. Exposure of the spent catalyst to ambient air at 25°C caused an increase of intensity of the above mentioned doublet.

When the reaction mixture was fed to an untreated oxidic catalyst at 25°C no changes in composition could be observed in the Mössbauer spectrum. Only after a prolonged time of reaction (25 h) at atleast 350°C a small fraction (18%) of the α-Fe_2O_3 was converted into Fe_3O_4. No indications were found for other iron compounds.

In Fig. 7, the Mössbauer spectra obtained for a more severely reduced catalyst are presented. The analysis data are shown in Table 2. After an 8-h reduction at 450°C, the spectrum of the α-Fe_2O_3 catalyst exhibited besides the characteristic sextuplet of α-Fe a strong unresolved background signal (spectrum A). (This background signal appeared to be a specific feature of the Fluka material since it was not found with BASF α-Fe_2O_3 material.) Exposure of the catalyst to the hydrogen–acetic acid mixture at 25°C for 72 h resulted in a complete conversion into iron(II) acetate as is evident from the well-resolved doublets in the spectrum (spectrum B). After subsequent increase in the reaction temperature to 350°C, the iron(II) acetate reacted to a mixture of Fe_3O_4 and α-Fe. Again, the α-Fe disappeared after prolonged time of reaction (spectra C to E). The major component in the spent catalyst is Fe_3O_4, with a small fraction of the yet unknown Fe(III) phase as indicated by the spectral contribution in the center of the spectrum. As observed for the partially reduced catalyst, the intensity of this Fe(III) phase was enhanced after exposure of the catalyst to ambient air.

Figure 8 shows the gas phase analysis during an experiment identical to that presented in Fig. 5, but now a flow

TABLE 2

Mössbauer Spectra Parameters, Reaction of Acetic Acid in 10% H_2 in He over α-Fe_2O_3

		T_m (°C)	IS (mm/s)	QS (mm/s)	H_{eff} (kOe)	Γ (mm/s)	SC (%)	Phase
A	α-Fe_2O_3, after prereduction (8 h, 450°C)	25	0.26	0.00	331	0.30	84	α-Fe
B	After 72 h exposure to acetic acid at 25°C	25	1.38	2.35	—	0.25	36	Fe(II) acetate
			1.55	2.23	—	0.28	64	Fe(II) acetate
C	Between 0 and 3.1 h reaction at 350°C	350	0.36	0.00	411	0.24	22	Fe_3O_4
			0.71	0.00	366	0.41	64	Fe_3O_4
			0.06	−0.01	302	0.21	14	α-Fe
D	After 3.1 h reaction at 350°C	25	0.55	0.00	491	0.27	31	Fe_3O_4
			0.94	0.00	460	0.35	63	Fe_3O_4
			0.26	−0.02	332	0.18	6	α-Fe
E	Between 3.1 and 11.4 h reaction at 350°C	350	0.34	0.00	411	0.31	33	Fe_3O_4
			0.71	0.00	367	0.34	67	Fe_3O_4
F	After 14.5 h reaction at 350°C	25	0.54	0.00	491	0.28	32	Fe_3O_4
			0.94	0.00	460	0.36	64	Fe_3O_4
			0.38	—	—	0.30	1	Fe^{3+} (?)
			0.68	—	—	0.30	1	Fe^{3+} (?)
			1.01	—	—	0.30	2	Fe^{3+} (?)

Note. The parameters are the same as those given in Table 1.

of 100% H_2 was used instead of 10% H_2 in He. Again a sharp, but now smaller, acetone peak was seen during the temperature rise. When the temperature of 350°C was reached, aldehyde, ethanol, and water were the only products found.

A series of Mössbauer experiments was also performed using 100% H_2 instead of 10% H_2 in Ar. The spectra were of the same quality as those presented in Figs. 6 and 7. Therefore, only the evaluation of them is presented in Table 3. Although the catalyst consisted of pure α-Fe before the reaction started, just a small amount of α-Fe was detected after 1 h of reaction on stream. The main part of the catalyst had become Fe_3O_4, while the remaining fraction contained both α-Fe and χ-Fe_5C_2 and some Fe(III). During the reaction, Fe_3O_4 and α-Fe were gradually converted to Fe_5C_2. After 17 h of reaction, the catalyst mainly contains χ-Fe_5C_2.

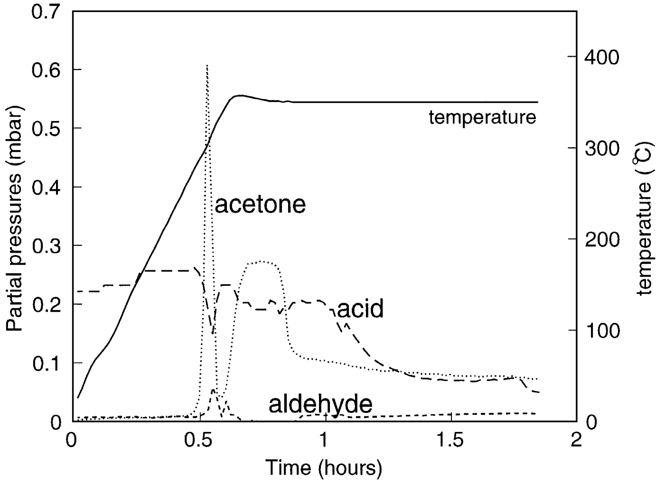

FIG. 5. The organic reaction products in a reaction of acetic acid in a 10% H_2 in He flow at 350°C over α-Fe_2O_3, which was prereduced 4 h at 450°C.

The Function of the Reductant

To clarify the role of hydrogen, two tests have been performed. First, hydrogen was replaced by an inert gas, viz.

TABLE 3

Mössbauer Spectra Parameters, Reaction of Acetic Acid in 100% H_2 over α-Fe_2O_3

		T_m (°C)	IS (mm/s)	QS (mm/s)	H_{eff} (kOe)	Γ (mm/s)	SC (%)	Phase
A	After 1 h reaction at 350°C	25	0.57	0.04	493	0.28	19.7	Fe_3O_4
			0.93	0.00	461	0.37	37.2	Fe_3O_4
			0.25	0.00	332	0.31	8.9	α-Fe
			0.46	0.00	201	0.52	19.3	Fe_5C_2
			0.75	0.24	120	0.43	7.2	Fe_5C_2
			0.61	0.70	—	0.46	4.3	Fe^{3+} (?)
B	After 17 h reaction at 350°C	25	0.54	0.00	490	0.30	0.4	Fe_3O_4
			0.93	0.00	460	0.35	1.8	Fe_3O_4
			0.49	−0.04	212	0.35	44.6	Fe_5C_2
			0.47	0.00	189	0.41	35.3	Fe_5C_2
			0.42	0.00	106	0.49	18.0	Fe_5C_2

Note. The parameters are the same as those given in Table 1.

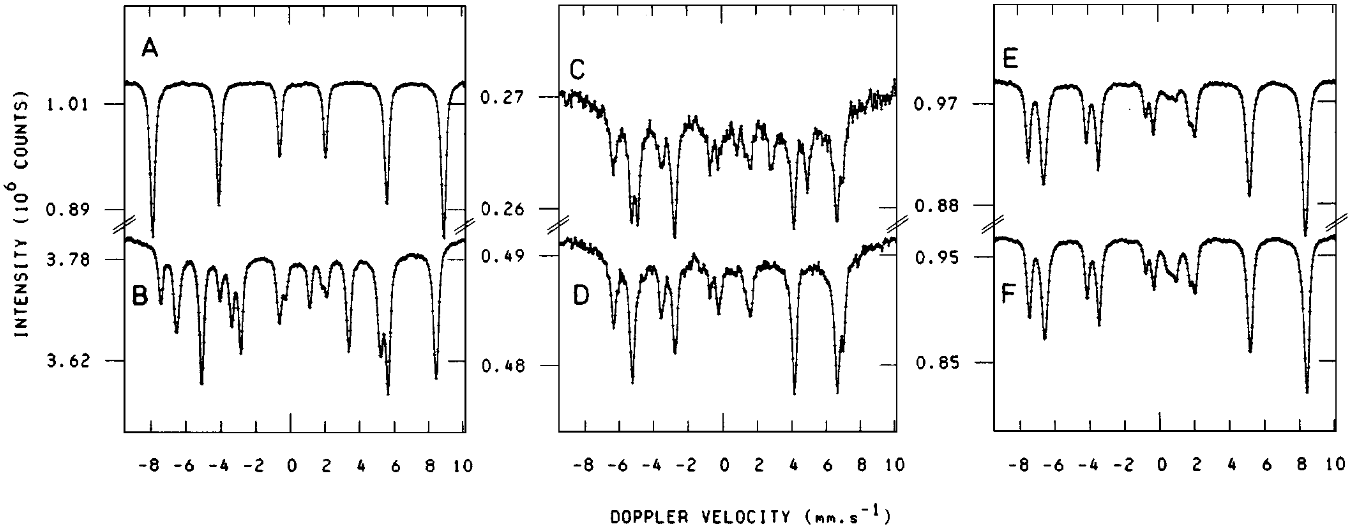

FIG. 6. Mössbauer spectra. Reaction of acetic acid in a 10% H_2 in He flow over α-Fe_2O_3, which was prereduced 4 h at 450°C. Reaction conditions comparable with those used in Fig. 5. Letters correspond to Table 1.

helium. Second, hydrogen was replaced by another reductant, viz. CO. The former experiment was done by switching the carrier gas from hydrogen to helium during a reaction over iron oxide at a constant temperature of 350°C (Fig. 9). In the presence of hydrogen, the reaction yielded mainly acetaldehyde, after the switch to helium no products were seen initially and, somewhat later, acetone was the main product, as can be seen in Fig. 9.

When the temperature-programmed experiment was performed in a CO flow instead of a hydrogen flow, no acetaldehyde but acetone was formed (Figs. 10). The reaction to acetone started at 350°C over the nonpretreated iron oxide (Fig. 10a). Over a catalyst prereduced with CO, the reaction started already at 250°C (Fig. 10b). When hydrogen was used to prereduce the iron oxide, but the reaction itself was performed in a CO flow, acetone was also the main product (Fig. 10c). The plot of the yield of acetone during the reaction resembles the decomposition pattern of $Fe(CH_3COO)_2OH$ (Fig. 10d). This is consistent with the mechanism of acetate formation and decomposition. The formation of acetate was observed when acetic acid was led over a reduced catalyst (see Fig. 8). This acetate formation causes also the decrease in the acetic acid signal at about 200°C seen in Fig. 10c (11), as acetic acid was consumed during the formation of the salt.

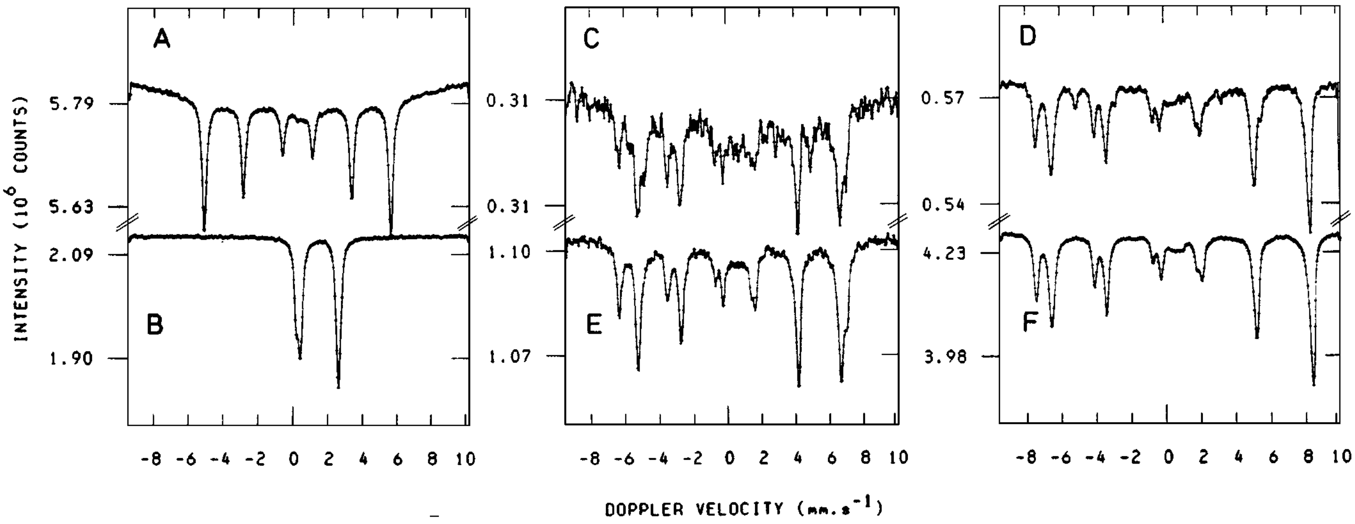

FIG. 7. Mössbauer spectra. Reaction of acetic acid in a 10% H_2 in He flow over α-Fe_2O_3, which was prereduced 8 h at 450°C. Letters correspond to Table 2.

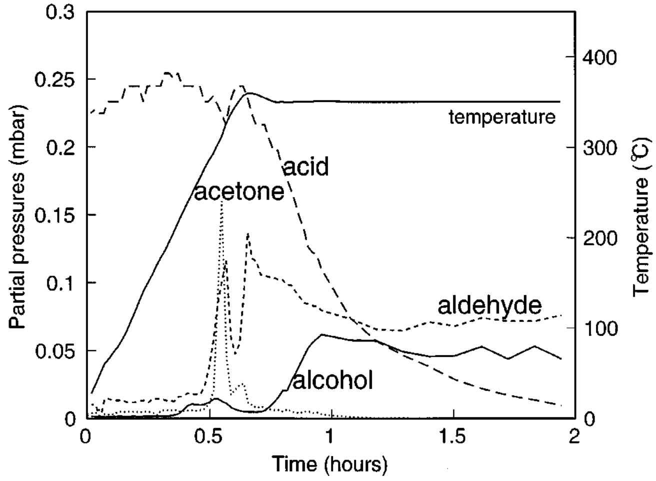

FIG. 8. Acetic acid and the organic reaction products over a prereduced α-Fe_2O_3 catalyst in a flow of 100% hydrogen at 350°C.

Comparison of Two Different α-Fe_2O_3 Catalysts

To test whether the high selectivity of the iron catalyst was characteristic of specifically the α-Fe_2O_3 used here or whether it was a common property of any α-Fe_2O_3, comparison was made between two catalysts. The α-Fe_2O_3 catalyst prepared by precipitation from a $Fe(NO_3)_3$ solution appeared to behave in the same way as the α-Fe_2O_3 obtained from Fluka. However, the prereduced forms of those catalysts did not behave in exactly the same way. The homemade oxide was a little less resistant to reaction temperatures above 400°C: it was slightly less active at the declining temperature trajectory. Nevertheless, during reactions at the constant temperature of 350°C, the catalyst kept its high activity and selectivity, just as the iron oxide obtained from Fluka.

DISCUSSION

Influence of the Pretreatment and Oxidation State during the Reaction

Iron oxide catalysts show a higher acetaldehyde production after being used once in a temperature-programmed reaction. Obviously, the catalyst gained its activity during the temperature-programmed reaction. By applying an adequate pretreatment procedure (simulating the modification of the catalyst during the reaction) the high level of activity and selectivity should be obtained already at the initial stage of the reaction. Of all pretreatments tested, only reduction had a positive influence on the selectivity. Prereduction at temperatures high enough to form metallic iron resulted in a higher acetaldehyde production (Fig. 3). The catalyst pretreated at 600°C had the highest selectivity and its XRD pattern showed only α-Fe. This could have meant that a selective catalyst consists of *only* metallic iron and that the oxide is completely inactive in the selective hydrogenation to acetaldehyde. However, these suggestions are in contradiction with the results obtained with Pt/titania catalysts as described in Ref. (10). Also, in a Pt/Sn system the oxide seemed to be important for the hydrogenation to acetaldehyde (8). This discrepancy is possibly caused by the fact that X-ray analysis is a technique, which is only sensitive to ordered bulk structures. As the catalytic reaction takes place on the surface, it is impossible to prove by XRD analysis alone what the active site looks like under reaction conditions.

During the reaction both reducing and oxidizing compounds react with the surface. Hydrogen and CO, which is occasionally formed during the reaction, are, of course, good reductants. Organic compounds, such as aldehydes, can also behave as reducing agents. Simultaneously, oxidizing compounds, such as CO_2, H_2O, and acetic acid, are present in the gas phase. Thus, it is conceivable that, when the steady state of the reaction is achieved, a steady state is established—with regard to the phase composition—caused by reduction and oxidation of the catalyst. This can result in a partly oxidized catalyst surface, even if the catalyst originally contained only metallic iron. Two earlier-reported facts support this idea: the relative ease of—partial—oxidation of iron at high temperatures by, e.g., water in the presence of hydrogen (21) and the difficulty to completely reduce iron oxide, either as a supported catalyst (22) or as a single crystal (23).

To test the possible existence of an oxidized phase on the iron surface during the reaction, even when the catalyst had been completely prereduced, TPR and Mössbauer analyses have been performed.

The TPR of a used Fe^0 catalyst showed a reduction peak (Fig. 4b), indicating that a partial oxidation of the catalyst by

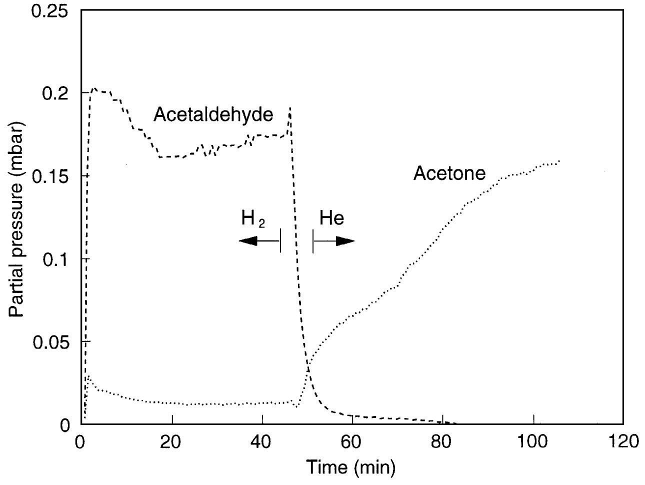

FIG. 9. Yield versus time at 350°C. The carrier gas was changed from hydrogen to helium halfway through the experiment.

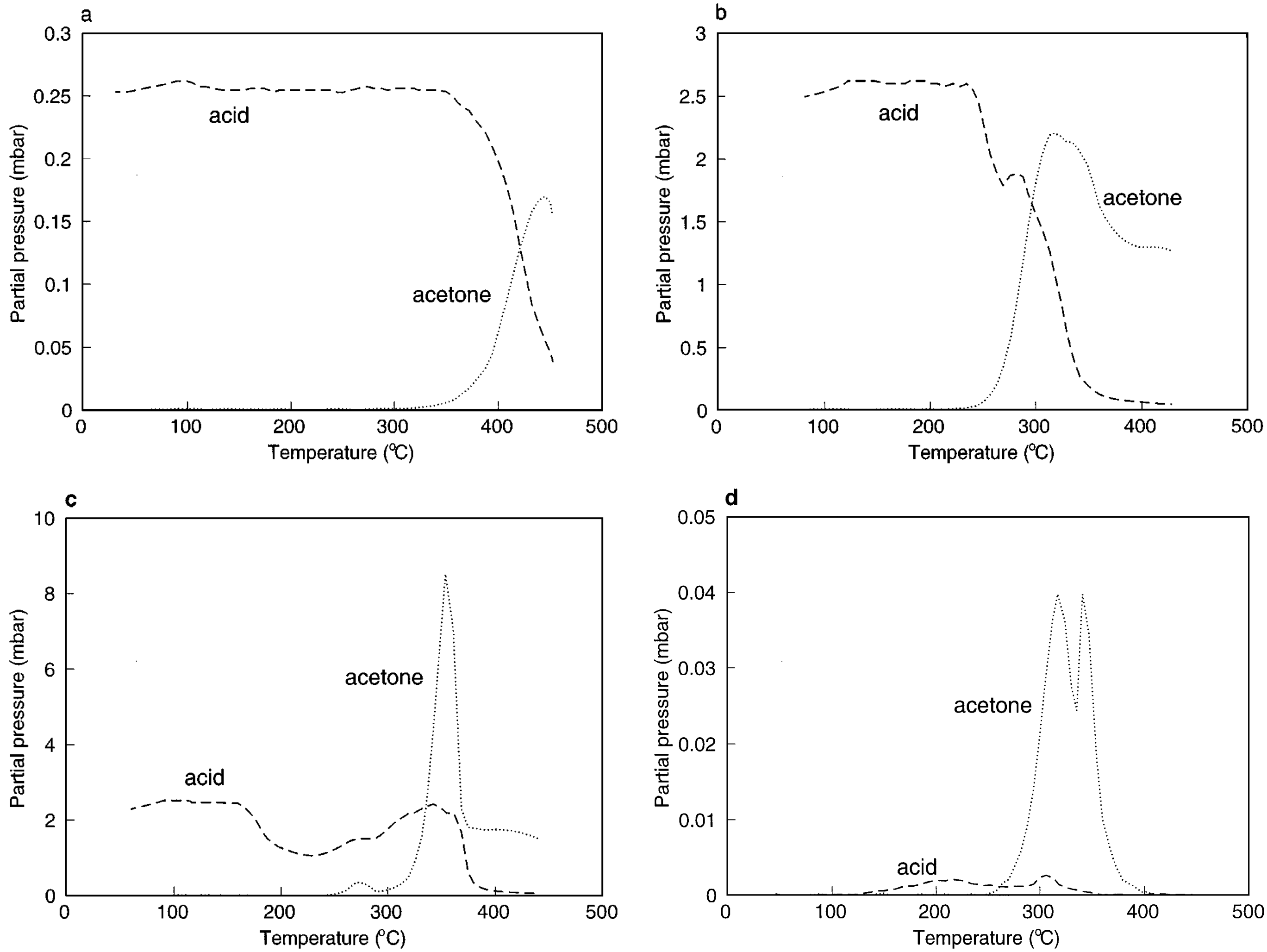

FIG. 10. (a) Reaction in a CO flow over unreduced iron oxide. (b) Reaction in a CO flow over iron oxide prereduced with CO. (c) Reaction in a CO flow over iron oxide prereduced with H_2. (d) Temperature-programmed decomposition of $Fe(CH_3COO)_2OH$ in He. In a–d all oxygenates formed during the increasing temperature part of the experiments are plotted.

the reaction mixture had indeed taken place. The position of the peak in the TPR spectrum is comparable with that of the reduction peak observed with a metallic iron catalyst, which had been oxidised by molecular oxygen (Fig. 4c). Thus, under reaction conditions an oxidic phase could be present, on which the selective hydrogenation to acetaldehyde takes place. The prereductioin of the catalyst up to α-Fe is then not needed to form the reaction site, but to provide a metallic phase, which is able to activate hydrogen (24, 25). Such picture is then in perfect compliance with the results obtained with other oxides and with the platinum-enriched oxides studied in reference (10).

Also the Mössbauer spectroscopy experiments indicate that a steady state is reached between oxidation and reduction of the catalyst. When 10% hydrogen in helium was used (hydrogen/acid ratio of about 4, as in various patents (14, 15)), the steady state shifted toward oxidation. Independently of the oxidation state of the catalyst at the start of the experiment, Fe_3O_4 was formed after 24 h of reaction (Figs. 6 and 7). This catalytic system appeared to be inactive in aldehyde formation (Fig. 5). When pure hydrogen was used without helium (hydrogen/acid ratio of about 40), the steady state of the catalyst reached during the steady-state reaction shifted toward a lower average oxidation state (Table 3). In this case, the catalyst appeared to be active in the desired aldehyde formation (Fig. 8). In the initial stage, α-Fe obviously is converted to Fe_3O_4 and χ-Fe_5C_2 when in contact with acetic acid. This is in agreement with the TPR results (Fig. 4b), which showed the presence of an oxidized phase, which caused the H_2O peak, and of a carbide, which caused the CH_4 peak. Later on, the spectral contribution of the iron carbide increases while the contributions of Fe_3O_4

and α-Fe decreases. As a consequence, the average oxidation state decreases during the reaction and is distinctly lower than the average oxidation state found during the reaction under 10% H_2. Nevertheless, Fe_3O_4 is still detected after 17 h. When an oxidic phase is present in a catalyst, which has been reduced, oxygen must be present at the surface. However, this oxidic phase cannot be the only phase exposed on the surface, as the pure iron oxide appeared to be inactive (Figs. 5 and 6). So probably not only an oxidized phase but also a zero-valent phase is simultaneously present in the exposed surface of an selective catalyst, as suggested in the Introduction and under Refs. (10, 13).

Both TPR and Mössbauer analysis confirm that completely prereduced iron catalysts are (partly) oxidized when brought into contact with an acetic acid-containing reaction mixture. The need of the presence of zero-valent iron, as shown by Fig. 3, is probably caused by the fact that some zero-valent metal must be present to activate molecular hydrogen. The picture developed for Pt/oxide systems (10) seems now to be in perfect compliance with the results presented here for iron oxide catalysts. In the former case platinum supplies activated hydrogen (as zero-valent iron does in the iron-based catalysts), and the actual selective deoxygenation reaction to acetaldehyde proceeds on the oxidic part of the catalyst via a Mars and Van Krevelen mechanism (10). This mechanism is shown schematically in Fig. 11: metallic iron activates hydrogen, which subsequently migrates to the oxide surface by a spillover mechanism. The spilled over hydrogen is used as a reactant in the hydrogenation reaction and to create vacancies needed for the Mars and Van Krevelen mechanism.

The differences mentioned in the Introduction between the results described under Refs. (14–17) and those described by Hindermann *et al.* (18, 19) can now be ascribed to the hydrogen/acid ratio used. The first authors used a ratio of 4 or less. Under these reaction conditions, the iron catalysts are oxidised to Fe_3O_4 as proved by Mössbauer spectroscopy, and therefore only ketonization products are found. However, Hindermann used a very high hydrogen/acetic acid ratio and, thus, managed to keep the catalyst partly reduced so that it could form acetaldehyde.

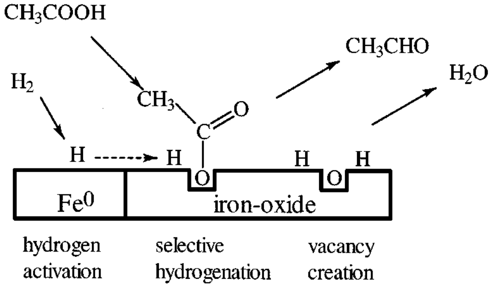

FIG. 11. Proposed reaction mechanism of the selective hydrogenation of acetic acid to acetaldehyde on iron catalysts.

The Function of the Reductant

Figure 9 shows indisputably that hydrogen is needed for the selective hydrogenation of acetic acid to aldehyde. Its function is at least twofold. First, hydrogen is required for keeping part of the catalyst sites in a reduced state during the steady state of the reaction. Second, it is consumed stoichiometrically in the reaction with acetic acid, since one molecule of acid reacts with one molecule of hydrogen to aldehyde and water.

Prereduction of the iron oxide catalyst enhances the activity. Comparison of Figs. 1 and 2 illustrates that the prereduced catalyst is more active: while in the first graph the reaction only just starts at 340°C, in the latter graph, the reaction is already at its maximum activity at this temperature. Also when the prereduction is done in a carbon monoxide atmosphere, it leads to a lower reaction temperature, as can be seen by comparing Fig. 10a with Fig. 10b. The reductant, however, is needed not only to activate the catalyst by prereduction, but also for the reaction of acetic acid to acetaldehyde. This could—in principle—proceed either via reaction [1] or [2].

$$CH_3COOH + CO \rightarrow CH_3CHO + CO_2 \qquad [1]$$

$$CH_3COOH + H_2 \rightarrow CH_3CHO + H_2O \qquad [2]$$

Since reaction [1], comprising an intramolecular hydrogen transfer, is never observed (no acetaldehyde is ever found when CO is the only reducing agent present) and reaction [2] regularly is, it is evident that specifically hydrogen is needed in the reduction of acetic acid to aldehyde. Furthermore, hydrogen is found to suppress the acetone formation, which is initiated by hydrogen abstraction and proceeds via ketene-like intermediates [10]. So, although both carbon monoxide and hydrogen can be used to activate the catalyst, only abundant hydrogen in the gas phase is able to make the reaction proceed selectively. The function of the hydrogen is thus at least twofold: it activates the catalyst by—partial—reduction, and it is a reactant in the selective hydrogenation of acetic acid. However, hydrogen likely has still another function. Figures 10c and 7 show that a well-reduced catalyst is very susceptible to the formation of acetates, which decompose to acetone, carbon dioxide, and iron oxide via reaction [3] (see also Fig. 10d).

$$Fe(CH_3COO)_2 \rightarrow CH_3COCH_3 + CO_2 + FeO \qquad [3]$$

The dip in the acetic acid signal seen in Fig. 10c, which is attributed to acetate formation, is also seen in Fig. 2. There it is remarkebly smaller. Perhaps, because the presence of hydrogen suppresses the salt formation by shifting the equilibrium of reaction [4] to the right.

$$Fe(CH_3COO)_2 + H_2 \rightleftarrows Fe^0 + CH_3COOH \qquad [4]$$

Hydrogen is, obviously, also needed to avoid a too deep oxidation of the iron. This explains why in Fig. 9, after switching off the hydrogen flow, no reactants are initially observed. The acid is probably first used to oxidize the iron and, once the catalyst is oxidized—either to iron acetate or to oxide—the acid reacts to acetone.

CONCLUSIONS

An iron-based catalyst can be very selective in the hydrogenation of acetic acid to acetaldehyde. Two conditions must be fulfilled to reach this high selectivity: the catalyst has to be prereduced in order to create a metallic phase, and the hydrogen/acid ratio must be high enough (viz. higher than four) to maintain a metallic phase during the reaction.

During the reaction, probably both the metallic and the oxidized phase are present. This is in accordance with the ideas developed previously for the Pt/oxide systems (10): the oxidized phase is the place of reaction and the metallic phase is the source of activated hydrogen. In this situation, the addition of platinum to an iron catalyst has indeed no effect, as there is already a metallic component (Fe^0) present to activate hydrogen.

The function of the reductant is twofold. It must keep the catalyst in its active reduced form and it has to react with acetic acid to give acetaldehyde. The last function cannot be fulfilled by carbon monoxide. A high hydrogen/acid ratio is, therefore essential.

REFERENCES

1. Maki, T., European Patent 0,150,961, 1985.
2. Van Geem, P. C., and Janssen, L. H. W., European Patent 0,290,096, 1988.
3. Hargis, D. C., U.S. Patent 4,950,799, 1990.
4. Strojny, E. J., U.S. Patent 4,328,373, 1982.
5. Maki, T., and Yokoyama, T., *Org. Synt. Chem.* **49**, 195 (1991).
6. Kondo, J., Ding, N., Maruya, K., Domen, K., Yokoyama, T., Fujita, N., and Maki, T., *Bull. Chem. Soc. Jpn.* **66**, 3085 (1993).
7. Yokoyama, T., Setoyama, T., Fujita, N., Nakajima, M., and Maki, T., *Appl. Cat. A.* **88**, 149 (1992).
8. Pestman, R., Koster, R. M., and Ponec, V., *Recl. Trav. Chim. Pays-Bas* **113**, 426 (1994).
9. Pestman, R., Van Duijne, A., Pieterse, J. A. Z., and Ponec, V., *J. Mol. Catal.* **103**, 175 (1995).
10. Pestman, R., Koster, R. M., Pieterse, J. A. Z., and Ponec, V., *J. Catal.* **168**, 255 (1997).
11. Pestman, R., Koster, R. M., Van Duijne, A., Pieterse, J. A. Z., and Ponec, V., *J. Catal.* **168**, 265 (1997).
12. Pestman, R., Ph.D. Thesis, Leiden, The Netherlands, 1995.
13. Grootendorst, E. J., Pestman, R., Koster, R. M., and Ponec, V., *J. Catal.* **148**, 261 (1994).
14. Wattimena, F., and Heijman, H. J., European Patent 0,101,111, 1984.
15. John, C. S., European Patent 0,178,718, 1986.
16. Kuriacose, J. C., and Jewur, S. S., *J. Catal.* **50**, 330 (1977).
17. Cressely, J., Farkhani, D., Deluzarche, A., and Kiennemann, A., *Mat. Chem. Phys.* **11**, 413 (1984).
18. Hindermann, J. P., Ph.D. Thesis, Strasbourg, France, 1981.
19. Hindermann, J. P., Kieffer, R., Bernier, J.-C., and Deluzarche, A., *J. Chem. Res. (M)* 4637/(*S*) 373 (1980).
20. Van der Kraan, A. M., and Niemantsverdriet, J. W., *in* “Industrial Applications of the Mössbauer Effect” (G. J. Long and J. G. Stevens, Eds.), p. 609. Plenum, New York, 1986.
21. Waugh, K. C., Butler, D., and Hayden, B. E., *Catal. Lett.* **24**, 197 (1994).
22. Wielers, A. F. H., Kock, A. J. H. M., Hop, C. E. C. A., Geus, J. W., and Van der Kraan, A. M., *J. Catal.* **117**, 1 (1989).
23. Vink, T. J., Der Kinderen, J. M., Gijzeman, O. L. J., and Geus, J. W., *Appl. Surf. Sci.* **26**, 367 (1986).
24. Ponec, V., Knor, Z., and Cerny, S., “Adsorption on Solids.” Butterworths, London, 1971.
25. Leibbrandt, G. W. R., and Habraken, F. H. P. M., *J. Catal.* **143**, 102 (1993).